Journal of Sound and Vibration (1999) **219**(2), 307–321
Article No. jsvi.1998.1885, available online at http://www.idealibrary.com.on IDEAL

A TRAVELLING WAVE APPROACH TO ACTIVE NOISE CONTROL IN DUCTS

J. YUAN AND K.-Y. FUNG

Department of Mechanical Engineering, The Hong Kong Polytechnic University, Hung Hom, Kowloon, Hong Kong

(*Received* 29 *April* 1997, *and in final form* 22 *July* 1998)

This paper presents a new scheme for active noise control (ANC) in ducts. It uses three pressure sensors to measure and separate the far field wave into the incident wave from the primary noise source, the reflected wave from the duct outlet, and the anti-sound wave generated by the loudspeaker. The transfer functions of wave components, measured between sensor locations, are simple delay factors with possible attenuation. The simple form of transfer functions makes it easier to design ANC schemes in practical applications. Applied to adaptive ANC, the adaptation process is simplified when the error path is equivalent to a delay factor. As a result, the new scheme identifies and compensates for the transfer function of the loudspeaker and the power amplifier without introducing an annoying pseudo random signal into the duct. Effectiveness of the scheme is demonstrated by direct time-domain numerical simulations.

1. INTRODUCTION

Various existing schemes of active noise control (ANC) in ducts may be classified into three approaches: the feedback control approach [1–5], the transfer function approach [6, 7], and the acoustic standing wave approach [8].

The first approach either decomposes the sound field into modal functions [1, 2], or derives state space matrices [3–5] to manage feedback from the pressure sensors. The controller then synthesizes the anti-sound signal to suppress the noise field. Controller performance is often subject to the accuracy of the system model matrices, which depend on the accuracy of either the modal functions or the impedances of the two duct ends. Some feedback controllers require measurement of the time derivative of the pressure signal, which is more expensive and susceptible to measurement and numerical errors.

The other two approaches synthesize feedforward cancellation signals according to a reference signal. The reference is either measured directly from the primary source [7] or measured betweeen the primary and secondary (antisound) sources [6, 8]. In the first case, the reference is independent of the antisound signal, and the only objective of the ANC is to match the transfer function of the duct and cancel the far field of the primary source [7]. In the second case, however, the

0022–460X/99/020307 + 15 $30.00/0

reference contains signals from both sources. The ANC should avoid the potential feedback effect of the secondary source as it attempts to cancel the effect of the primary source [6, 8].

An important advantage of a feedforward ANC is its ability to improve performance by adaptation [9, 10]. Using an acoustic standing wave model, Munjal and Eriksson find that an optimal feedforward ANC is independent of the model of the duct [8]. Instead, it only depends on the acoustic impedance of the secondary source. Once an adaptive law drives the convergence of a feedforward ANC to optimum, the performance of the optimal ANC will not be affected by the change of impedance of any ends of the duct [8].

The key to the convergence of an adaptation process is the error signal. For a feedforward ANC, this signal reflects the far field cancellation effect. It is measured by a pressure sensor placed downstream a distance away from the secondary source. The accuracy of the adaptation depends on the accuracy of the transfer function of the error path, which transfers the cancellation effect from the secondary source to the error sensor. Unfortunately, the transfer function of the error path is a function of the impedance of the duct outlet. While it is possible to identify the transfer function of the error path on-line, the side effect is adding a pseudo random signal to the antisound that could not be cancelled.

The pseudo random signal excites the impulse response of the error path that, in turn, joins the cancellation error to form a propagating mixture. The adaptive law has to process the signal from the error sensor in order to separate the impulse response from the cancellation error. There exists an inherent inaccuracy when one tries to separate two signals sharing the same frequency range without an *a priori* knowledge. Such an inaccuracy causes inaccuracy in the estimated transfer function of the error path that, in turn, causes inaccuracy to the ANC transfer function.

This paper presents a new approach to feedforward ANC in ducts. It places an additional pressure sensor near the primary error sensor, enabling the separation of travelling waves from the acoustic pressure signals. The available wave components are the incident wave from the primary source, the reflected wave from the duct outlet, the error wave and the antisound wave due to the secondary source. For one-dimensional wave propagation problems, the transfer functions of travelling waves are simple delay factors with possible attenuation. An acoustic duct can be approximated by a one-dimensional wave system when its cross-section area is much smaller than the wave length of the noise. The separation of travelling waves thus simplifies problems associated with transfer functions of duct sections. The adaptation process becomes simpler. It becomes possible to identify the transfer function of the error path, the loudspeaker, and power amplifier without the annoying pseudo random signal.

The rest of this paper is organized as follows: section 2 explains the system set-up and the separation of travelling waves. The proposed ANC is presented in section 3. Section 4 addresses the issue of system identification, and section 5 compares the proposed method with those available in the literature. Simulation results are given in section 6 to illustrate the performance of the proposed system. A brief conclusion is given in section 7.

2. TRAVELLING WAVE SEPARATION

The proposed system is very similar to those presented in [7–10], except for the additional pressure sensor placed near the downstream primary error sensor. Figure 1 illustrates locations of the sensors and the travelling wave components. A loudspeaker is placed at $x_s = 0{\cdot}0$ as the secondary source. The primary source is sufficiently far away from the zone such that the noise can be considered to be coming from negative infinity. Three pressure sensors, labelled as s_1, s_2 and s_3 respectively, are placed at co-ordinates $x_1 = -l_1$, $x_2 = l_2$ and $x_3 = l_2 + l_3$ respectively. The upstream sensor s_1 should be placed in such a way that $x_1 = -l_1$ is not a node of the standing waves. This restriction is required to avoid a potential situation where some standing waves exist before the ANC adapts to its optimal state. There are generally no other restrictions on the co-ordinates of the sensors. A choice of $l_1 = l_2$, however, would simplify the separation of travelling waves, as shown later. The sensors pick up pressure signals p_1, p_2 and p_3. These signals are used either to synthesize the antisound signal or to identify the optimal ANC transfer function.

It is assumed that the duct is a linear wave propagating system. The principle of superposition enables one to study the waves according to their sources of origin. The incident wave comes from negative infinity and travels in the positive direction. It is a function of time and space. If one uses w_p to denote the incident wave at x_1, then the incident wave is $w_p\, e^{-jk(l_1 + l_2)}$ at x_2 and $w_p\, e^{-jk(l_1 + l_2 + l_3)}$ at x_3. Here subscript p indicates a wave from the *primary* source; $e^{-jk(l_1 + l_2)}$ is a delay factor with possible attenuation depending on whether the wave number k is real or complex.

The reflected wave is denoted by w_r, where subscript r indicates that the wave is due to *reflection*. This signal, sampled at x_2, travels in the negative direction. It becomes $w_r\, e^{-jk(l_1 + l_2)}$ when sampled at x_1.

The antisound wave, generated by the secondary source (loudspeaker), travels in both directions. Only the far field effects of the antisound are considered here. Let $p_s(x, t)$ and $v_s(x, t)$ denote, respectively, the pressure and velocity signals due to the *secondary* source. It is well known that p_s is spatially symmetric and v_s spatially antisymmetric with respect to the secondary source, or mathematically,

$$p_s(x - x_s, t) = p_s(x_s - x, t), \qquad v_s(x - x_s, t) = -v_s(x_s - x, t), \qquad (1, 2)$$

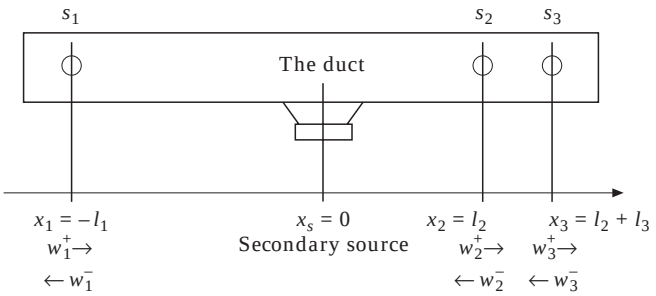

Figure 1. Travelling waves in a duct.

where x_s is the co-ordinate of the secondary source. In this study, $x_s = 0{\cdot}0$ for simplicity, hence p_s is spatially an even function and v_s spatially an odd function.

By introducing $Y_o = c_o/S$, where c_o is the speed of sound and S the area of cross-section of the duct, the foward and backward waves of the secondary source can be expressed as

$$w_s^+(x, t) = Y_o v_s(x, t) + p_s(x, t), \qquad w_s^-(x, t) = Y_o v_s(x, t) - p_s(x, t),$$

respectively. It is not difficult to see, from (1) and (2), that w_s^+ and w_s^- are both spatially antisymmetric with respect to the secondary source. With $x_s = 0{\cdot}0$, one can verify that

$$w_s^-(-l_2, t) = -w_s^+(l_2, t) = -w_s, \tag{3}$$

where w_s represents the forward anti-sound wave at $x_2 = l_2$ while $-w_s$ the backward antisound wave at $x = -l_2$. In other words,

$$w_s^-(x_1, t) = w_s^-(-l_1, t) = -w_s\, \mathrm{e}^{\mathrm{j}k(l_2 - l_1)}, \tag{4}$$

at $x_1 = -l_1$. The argument of $\mathrm{e}^{\mathrm{j}k(l_2 - l_1)}$ reflects the spatial difference between co-ordinates $-l_1$ and l_2. It is a delay factor if $l_1 > l_2$ or a lead factor if $l_2 \geqslant l_1$.

The focus can now be directed to the three spots where the pressure sensors are mounted. Let w_1^+, w_2^+ and w_3^+ denote, respectively, the forward travelling waves sampled at these spots; and let w_1^-, w_2^- and w_3^- denote the corresponding backward travelling waves. At $x_1 = -l_1$, the incident wave from the primary source is the only wave that travels in the positive direction when the coordinate of primary source is negative infinity. In a real application where the duct length is finite, the incident wave may include the wave from the primary source and the reflection from the negative end of the duct. Regardless of its origins, the entire incident wave must be cancelled by the antisound. For this reason, the upstream incident wave is considered to be from one single noise source defined as w_p at x_1, or

$$w_1^+ = w_p. \tag{5}$$

The reflected wave from the duct outlet and the secondary source constitute the backward travelling wave,

$$w_1^- = w_r\, \mathrm{e}^{-\mathrm{j}k(l_1 + l_2)} - w_s\, \mathrm{e}^{\mathrm{j}k(l_2 - l_1)}, \tag{6}$$

where (4) has been used to replace $w_s^-(-l_1, t)$.

The forward travelling wave at $x_2 = l_2$, denoted as w_2^+, has two components: the incident noise and the antisound intended to cancel the noise. This is actually the error signal. On the other hand, there is only one component in w_2^-, that is the reflection from the duct outlet. The two waves are given by

$$w_2^+ = w_p\, \mathrm{e}^{-\mathrm{j}k(l_1 + l_2)} + w_s \quad \text{and} \quad w_2^- = w_r. \tag{7}$$

Similarly, the two travelling waves at $x_3 = l_2 + l_3$ can be written as

$$w_3^+ = w_p\, \mathrm{e}^{-\mathrm{j}k(l_1 + l_2 + l_3)} + w_s\, \mathrm{e}^{-\mathrm{j}kl_3} \tag{8}$$

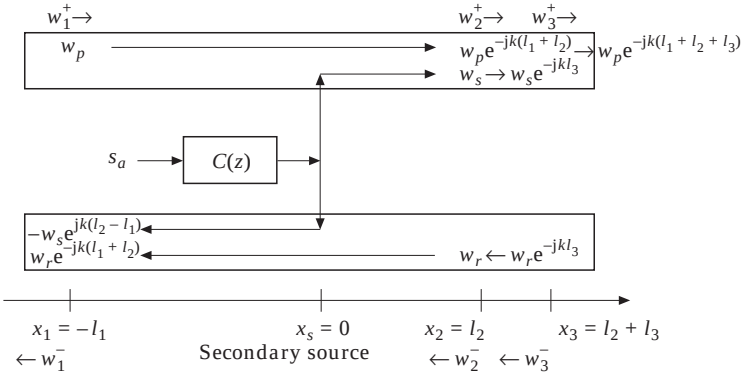

Figure 2. The forward and backward waves.

and

$$w_3^- = w_r \, e^{jkl_3}. \tag{9}$$

Figure 2 illustrates the locations where w_p, w_s and w_r are sampled and their contributions to the travelling waves at different spots. The secondary source is represented by a signal $C(z)s_a$ that will be explained in the next section.

The sensors are assumed to be omnidirectional microphones, which measure the acoustic pressure of the sound field. According to equations (5–9), the pressure signals have the following expressions

$$p_1 = \tfrac{1}{2}(w_p - w_r \, e^{-jk(l_1+l_2)} + w_s \, e^{jk(l_2-l_1)}), \tag{10}$$

$$p_2 = \tfrac{1}{2}(w_p \, e^{-jk(l_1+l_2)} + w_s - w_r), \tag{11}$$

$$p_3 = \tfrac{1}{2}(w_p \, e^{-jk(l_1+l_2+l_3)} + w_s \, e^{-jkl_3} - w_r \, e^{jkl_3}) \tag{12}$$

which are simplified for determination of the forward, reflected and antisound waves. Combining (7, 11, 12), one obtains

$$w_2^+ = \frac{2}{1 - e^{-j2kl_3}} (p_2 - p_3 \, e^{-jkl_3}), \tag{13}$$

$$w_r = \frac{2}{1 - e^{-j2kl_3}} (p_2 \, e^{-j2kl_3} - p_3 \, e^{-jkl_3}), \tag{14}$$

$$w_p = [2p_1 - 2p_2 \, e^{jk(l_2-l)} - w_r \, e^{jk(l_2-l_1)}(1 - e^{-j2kl_2})]/(1 - e^{-j2kl_1}), \tag{15}$$

and

$$w_s = [2p_2 - 2p_1 \, e^{-jk(l_1+l_2)} + w_r(1 - e^{-j2k(l_1+l_2)})]/1 - e^{-j2kl_1}. \tag{16}$$

There is no loss of generality to assume the simplified form of (15) and (16) by letting $l_1 = l_2 = l$, i.e.,

$$w_p = 2 \frac{p_1 - p_2}{1 - e^{-j2kl}} - w_r, \qquad w_s = 2 \frac{p_2 - p_1 \, e^{-j2kl}}{1 - e^{-j2kl}} + w_r(1 + e^{-j2kl}). \tag{17, 18}$$

This choice will be used from here on for simplicity.

3. ACTIVE NOISE CONTROL

Unlike other ANC schemes in the literature, the objective of this study is to make $w_2^+ \to 0$. Since w_2^+ is the forward travelling wave at $x_2 = l_2$, it convergence to zero means no more noise propagating towards the outlet starting from x_2. When that happens, w_r only represents the environment noise from outside of the duct outlet. There is no need for the ANC to deal with it.

The proposed ANC system is represented by a block diagram in Figure 3, where the duct is represented by the dashed box. The ANC synthesizes a signal s_a that passes through the power amplifier and the loudspeaker to excite the sound field. The far field antisound wave reaches point $x_2 = l_2$ after a delay of e^{-jkl_2}. An analytical description of the delay is a Laplace transform $e^{-jkl_2} \to e^{-sl_2/c}$ which is equivalent to a Z-transform $e^{-sl_2/c} \to z^{-N_2}$ if the delay is an exact integer number of sample intervals [12]. Let w_s denote the antisound measured at $x_2 = l_2$ and $C(z)$ the total transfer function of the power amplifier plus loudspeaker. On can express w_s as

$$w_s = C(z)s_a z^{-N_2}. \tag{19}$$

In this study, $C(z)$ is called the transfer function of the excitation path. Its effect is similar to $H_{sa}(z)$ in [6] and the acoustic impedance Z_{sa} in [8]. This transfer function can be either measured off-line or identified on-line, since w_s and s_a are available in the present system.

Let $H(z) = s_a/w_p$ denote the transfer function of the ANC. Substituting into (19), one obtains

$$w_s = C(z)H(z)w_p z^{-N_2}. \tag{20}$$

This equation describes the passage of w_p, through the ANC $H(z)$, the excitation path $C(z)$ and the Z-transform delay of z^{-N_2}, before arriving at x_2. According to (7), $w_2^+ \to 0$ implies $w_s \to -w_p e^{-jk(l_1 + l_2)}$. With another Z-transform delay ($e^{-jkl_1} \to e^{-sl_1/c} \to z^{-N_1}$, assuming that the delay is another exact integer number of sample intervals), the objective to $w_s \to -w_p z^{-(N_1 + N_2)}$ implies

$$C(z)H(z)w_p z^{-(N_1 + N_2)} \to -w_p z^{-(N_1 + N_2)}.$$

Obviously, the transfer function of ANC should be chosen in such a way that, at convergence, the above expression becomes an equality, or

$$H(z) = -T(z)z^{-N_1} \quad \text{and} \quad T(z) = 1/C(z). \tag{21}$$

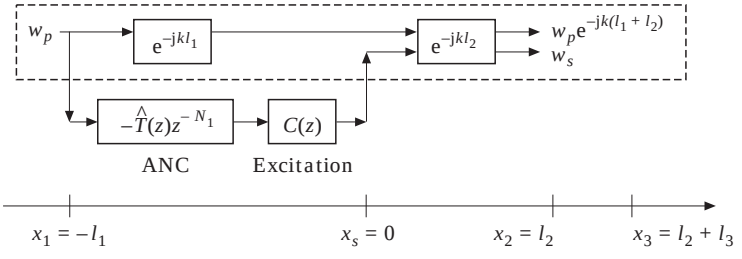

Figure 3. Block diagram of the ANC system.

A further substitution of (14) and (17) suggests that the ANC should synthesize s_a by

$$s_a = -\frac{z^{-N_1}}{\hat{C}(z)} w_p = -\frac{2z^{-N_1}}{\hat{C}(z)} \left(\frac{p_1 - p_2}{1 - z^{-2N_1}} - \frac{p_2 z^{-2N_3} - p_3 z^{-N_3}}{1 - z^{-2N_3}} \right), \tag{22}$$

where z^{-N_3} is the Z-transform of e^{-jkl_3} and $\hat{C}(z)$ is an estimation of $C(z)$ either from an on-line adaptation algorithm or from the exact form of $C(z)$ if available. According to (22), it is computationally more convenient to synthesize s_a using the intermediate signal w_p, which can be seen as a filtered version of pressure signals p_1, p_2 and p_3.

4. SYSTEM IDENTIFICATION

There is an uncertain function in (22)—the estimated transfer function of the excitation path $\hat{C}(z)$. This section considers a practical situation where the exact form of $C(z)$ is not available and the focus is how to obtain $\hat{C}(z)$. While it is possible to measure the electronic transfer function of the power amplifier and the loudspeaker with satisfactory accuracy, it is not so convenient to measure the acoustical transfer function that describes the wave–source relation. Even if $\hat{C}(z)$ is available by measurement, one still cannot simply substitute $\hat{C}(z)$ into (22) since $\hat{C}(z)$ may not necessarily be a minimum phase approximation of $C(z)$. If $\hat{C}(z)$ is non-minimum phase, then $1/\hat{C}(z)$ is unstable and useless.

The adaptive technique provides an effective solution to this problem. A properly designed adaptation algorithm can help the ANC to learn by trial and error. Starting with an initial ANC transfer function $H(z)$, the adaptive law adjusts the coefficients of $H(z)$ according to the cancellation error signal, such that the system converges to an optimal state in the least mean square (LMS) error sense. The well known LMS algorithm identifies a linear system as a linear difference equation. An important step in the design of an adaptive law is to find a pair of input/output signals and decide what is the error signal to be minimized. For the proposed ANC system, there are two methods to identify the excitation path $C(z)$. The two methods minimize two different error signals, detailed as follows.

4.1. INDIRECT IDENTIFICATION

This method uses w_s as the input and $s_a z^{-N_2}$ as the output signal, which are available by (18) and (22) respectively. The LMS algorithm can be expressed as

$$\min_{\hat{T}(z)} \| s_a z^{-N_2} - \hat{T}(z) w_s \| = \min_{\hat{T}(z)} \| (1 - \hat{T}(z) C(z)) s_a z^{-N_2} \|, \tag{23}$$

where (19) has been substituted for w_s. According to (23), the process minimizes a weighted norm of $1 - \hat{T}(z)C(z)$ with the spectrum of $s_a z^{-N_2}$ as the weighting function. At convergence, it obtains a stable (but not necessarily minimum phase) approximation $\hat{T}(z) \to 1/C(z)$, by-passing the inverse of $\hat{C}(z)$ and the minimum phase problem.

The indirect method, while being simple and requiring only one adaptation process, does not minimize the cancellation error w_2^+. There is no analytical

measure to see how well the convergence of (23) affects $\|w_2^+\|$. This drawback calls for the second method that requires two LMS processes to achieve the objective of minimizing $\|w_2^+\|$.

4.2. DIRECT IDENTIFICATION

As its name stands, the objective of this method is

$$\begin{aligned}\min_{\hat{T}(z)} \|w_2^+\| &= \min_{\hat{T}(z)} \|w_p z^{-(N_1+N_2)} + w_s\| = \min_{\hat{T}(z)} \|[1 - C(z)\hat{T}(z)]w_p z^{-(N_1+N_2)}\| \\ &= \min_{\hat{T}(z)} \|[1 - \hat{T}(z)C(z)]w_p z^{-(N_1+N_2)}\| = \min_{\hat{T}(z)} \|w_p z^{-(N_1+N_2)} - \hat{T}(z)y\|,\end{aligned} \tag{24}$$

where $y = C(z)w_p z^{-(N_1+N_2)}$ is the "filtered-x signal". Transfer functions $\hat{T}(z)$ and $C(z)$ are commutable since these are linear transfer functions. The minimization described by (24) is not possible when $C(z)$ is not available. The unknown nature of $C(z)$ prohibits the synthesis of y as the input signal to the LMS process. One possible way to get around is to substitute

$$\hat{y} = \hat{C}(z)w_p z^{-(N_1+N_2)},$$

where $\hat{C}(z)$ is available by the first LMS process. This process uses w_s as the output, $s_a z^{-N_2}$ as the input, and minimizes

$$\min_{\hat{C}(z)} \|w_s - \hat{C}(z)s_a z^{-N_2}\| = \min_{\hat{C}(z)} \|[C(z) - \hat{C}(z)]s_a z^{-N_2}\|. \tag{25}$$

Its purpose is to estimate the filtered-x signal $\hat{y} = \hat{C}(z)w_p z^{-(N_1+N_2)}$. The resultant $\hat{C}(z)$ should be a stable (but not necessarily minimum phase) approximation of $C(z)$, a straightforward task for the available LMS techniques.

It should be emphasized that $\hat{T}(z)$ is not a simple inverse filter $1/\hat{C}(z)$ here. The adaptation of $\hat{T}(z)$ is, in fact, the job of a second LMS process

$$\min_{\hat{T}(z)} \|w_p z^{-(N_1+N_2)} - \hat{T}(z)\hat{y}\|, \tag{26}$$

which obtains a stable but not necessarily minimum phase $\hat{T}(z)$. Before the convergence of $\hat{y} \to y$, the accuracy of $\hat{y}$ would affect the accuracy but **not** stability of $\hat{T}(z)$ as long as $\hat{y}$ and w_p are bounded, which is not a problem when $\hat{C}(z)$ is stable. Like the indirect method, this one also by-passes the inverse of $\hat{C}(z)$ and the minimum phase problem. The two LMS processes, (25) and (26), combine to form an upper bound on the intended objective (24) as follows

$$\begin{aligned}\min_{\hat{T}(z)} \|w_2^+\| &= \min_{\hat{T}(z)} \|w_p z^{-(N_1+N_2)} - \hat{T}(z)\hat{y} + \hat{T}(z)\hat{y} + w_s\| \\ &\leqslant \min_{\hat{T}(z)} \|w_p z^{-(N_1+N_2)} - \hat{T}\hat{y}\| + \min_{\hat{T}(z)} \|\hat{T}\hat{y} + Cs_a z^{-N_2}\| \\ &\leqslant \min_{\hat{T}(z)} \|w_p z^{-(N_1+N_2)} - \hat{T}\hat{y}\| + \min_{\hat{C}(z)} \|[C - \hat{C}]s_a z^{-N_2}\|,\end{aligned} \tag{27}$$

where (16) has been substituted for w_s while

$$\hat{T}(z)\hat{y} = \hat{T}(z)\hat{C}(z)w_p z^{-(N_1+N_2)} = -\hat{C}(z)s_a z^{-N_2},$$

since the linear transfer functions $\hat{T}(z)$ and $\hat{C}(z)$ are also commutable.

Figure 4 plots the block diagram of the adaptive ANC system. The two LMS processes are represented by two boxes marked with mathematical norms. The

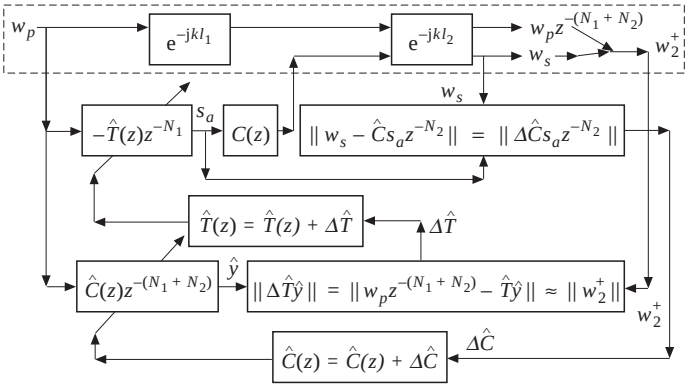

Figure 4. Block diagram of the adaptive ANC system.

output of the two LMS boxes are $\Delta\hat{C}$ and $\Delta\hat{T}$ respectively. The system uses the fresh versions of $\Delta\hat{C}$ and $\Delta\hat{T}$ to update the ANC at a rate K times slower than the system sampling rate.

The adaptations are designed to avoid inter-coupling between the two processes (25) and (26). Before the convergence of the system, s_a may not necessarily excite $C(z)$ correctly to provide a right version of w_s for effective cancellation of $w_p z^{-(N_1+N_2)}$. Yet s_a and w_s are input/output signals of the physical excitation path $C(z)$. These two signals are used to identify a casual and stable $\hat{C}(z)$ by (25), regardless of cancellation effect $w_s + w_p z^{-(N_1+N_2)}$. With guaranteed stability of $\hat{C}(z)$, the filtered-x signal $\hat{y} = \hat{C}(z)w_p z^{-(N_1+N_2)}$ is bounded since the incident noise wave w_p is bounded. A stable $\hat{y}$ helps (26) to minimize $\|w_2^+\|$ and identify a stable (but not necessarily minimum phase) $\hat{T}(z)$. While (26) depends on $\hat{y}$ which, in turn, depends on (25), (25) itself is independent of any other processes.

Since $\hat{T}(z)$ is not a simple inverse filter $1/\hat{C}(z)$, the system allows certain estimation error. In particular, it works with causal and stable estimates $\hat{T}(z)$ and $\hat{C}(z)$ when both are not necessarily minimum phase. The convergence of two separate LMS processes together minimizes $\|w_2^+\|$ as suggested by (27).

5. COMPARISON WITH OTHER METHODS

The proposed ANC synthesizes a feedforward signal to cancel the unwanted noise. The control signal is based on a reference that contains both the incident noise and the antisound wave—a more realistic model than those that assume the absence of antisound in the reference. Under such an assumption, the ANC has to avoid the feedback effect of the antisound while attempting to cancel the noise. For these ANC schemes two excellent results were reported by Elliot and Nelson [6] and Munjal and Eriksson [8]. The present method provides two improvements with respect to their results.

5.1. DYNAMIC RANGE

Let s_a and p_1 denote, respectively, the ANC signal and the pressure signal of the up-stream sensor. For the conditions used in this study, the ANC of Elliot and

Nelson [6] synthesizes s_a by

$$s_a = -(1/H_{sa})(z^{-N_1}/[1 - z^{-2N_1}])p_1, \tag{28}$$

where H_{sa} is the transfer function of the secondary source that includes the power amplifier, the loudspeaker, and the acoustic pressure–source relation. The ANC of Munjal and Eriksson [8], on the other hand, synthesizes s_a by

$$s_a = -(Z_{sa}/Y_o)(z^{-N_1}/[1 - z^{-2N_1}])p_1, \tag{29}$$

where Z_{sa} is the acoustic impedance of the secondary source. The proposed ANC synthesizes s_a by

$$s_a = -\frac{2z^{-N_1}}{C(z)}\left(\frac{p_1 - p_2}{1 - z^{-2N_1}} - \frac{p_2 z^{-N_3} - p_3}{1 - z^{-2N_3}}\, z^{-N_3}\right), \tag{30}$$

where $l_1 = l_2$ has been assumed.

All three ANC schemes apply the same filter $z^{-N_1}/(1 - z^{-2N_1})$ to pressure signal p_1. This seems to be a common way to avoid the feedback effects of the antisound. Yet there exists a significant difference between the proposed method and the result of Elliot and Nelson [6] and that of Munjal and Eriksson [8]. The difference is hidden in the filter $z^{-N_1}/(1 - z^{-2N_1})$ operation, which is unstable with $2N_1$ poles evenly distributed on the unit circle. In practice, it must be replaced by a stable filter $z^{-N_1}/(1 - \gamma z^{-2N_1})$ where $0 < \gamma < 1$. The substitute has $2N_1$ poles in the complex Z-plane at $\exp(jk\pi/N_1)\gamma^{1/2N_1}$ for $0 \leqslant k \leqslant 2N_1 - 1$, corresponding to resonant peaks of magnitude $1/(1 - \gamma)$ (when $z^{2N_1} = 1$) and valleys of magnitude $1/(1 + \gamma)$ (when $z^{2N_1} = -1$).

The peaks and valleys spread evenly in the working frequency band. The ANC must maintain high linearity for all peaks and valleys alike in order to cancel the noise without creating unwanted high order harmonics. Its dynamic range may be measured by the magnitude ratio of the highest peak and lowest valley, which is $20 \log \{(1 + \gamma)/(1 - \gamma)\}$. Clearly, the larger $20 \log \{(1 + \gamma)/(1 - \gamma)\}$ is, the more expensive the ANC hardwares. A practical implementation of ANC would certainly include a power amplifier and a loudspeaker whose costs go up drastically as the linearity requirement and dynamic range increase. From this point of view, one would like to keep γ to a minimum.

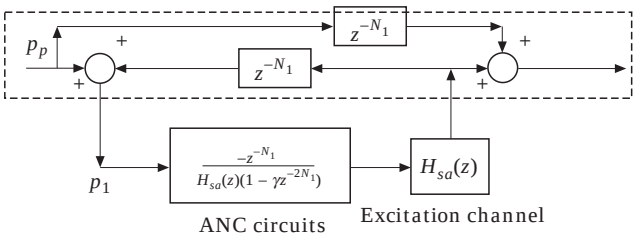

Figure 5. Block diagram of imperfect ANC cancellation.

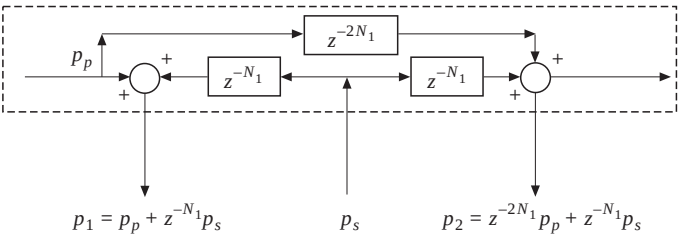

Figure 6. Pressure signals in a long duct.

On the other hand, γ should be close to 1 as much as possible to have good noise cancellation as explained by Figure 5, the block diagram of the ANC system proposed by Elliot and Nelson [6]. They considered long ducts with negligible reflections, assumed the pressure signal propagates with pure time delays, and excluded the near field effects of the loudspeaker to derive (28). The duct is an analog system with a continuous delay factor e^{-jkl_1}, which is equivalent to a discrete delay factor z^{-N_1} when synchronized with the digital ANC system. The upstream sensor picks up primary noise pressure p_p and a delayed feedback of antisound pressure $z^{-N_1}p_s$. Both signals enter the ANC to generate the antisound $p_s = H_{sa}(z)[-1/H_{sa}(z)]\,[z^{-N_1}/(1-\gamma z^{-2N_1})](p_p + z^{-N_1}p_s)$. The downstream pressure, depending on the measurement location, should be either $z^{-N_1}p_n + p_s$ or its delayed version. A block diagram reduction reveals that the resultant cancellation is given by

$$z^{-N_1}p_p + p_s = \{(1-\gamma)z^{-N_1}/[1+(1-\gamma)z^{-2N_1}]\}p_p. \tag{31}$$

It indicates a perfect cancellation if $\gamma = 1$ (which is impossible due to stability reasons) and if the ANC consists of perfectly linear circuits (which is very expensive). A similar conclusion can be arrived for the ANC structure of (29).

One thus faces a dilemma, i.e., small dynamic range of ANC or ineffective cancellation (31). The final trade-off is a γ as close to 1 as allowed by the dynamic range and linearity of the ANC hardware.

The proposed method avoids such a problem. For long ducts with negligible reflections from the duct outlet, only two sensors are needed instead of three. The sensor placement is shown in Figure 6 where the upstream and downstream sensors sandwich the antisound loudspeaker with equal distances. The long duct is represented by the dash-lined box. Assuming perfect synchronization, the analog delay factors inside the duct can be treated as equivalent discrete delay factors. Let p_1 and p_2 denote, respectively, the pressure signals measured by the upstream and downstream sensors. Figure 6 shows that $p_1 = p_p + z^{-N_1}p_s$ and $p_2 = z^{-2N_1}p_p + z^{-N_1}p_s$. Immediately, one knows how to separate the primary sound pressure

$$\tilde{p}_p = (p_1 - p_2)/[1-\gamma z^{-2N_1}] = [(1-z^{-2N_1})/(1-\gamma z^{-2N_1})]p_p \tag{32}$$

from the secondary (antisound) pressure

$$z^{-N_1}\tilde{p}_s = \frac{p_2 - z^{-2N_1}p_1}{1-\gamma z^{-2N_1}} = \frac{1-z^{-2N_1}}{1-\gamma z^{-2N_1}}\,z^{-N_1}p_s. \tag{33}$$

The above equations imply $\tilde{p}_p \approx p_p$ and $\tilde{p}_s \approx p_s$ when $\gamma \approx 1$. As with wave signals w_p and w_s, pressure signals $\tilde{p}_p$ and $z^{-N_1}\tilde{p}_s$ can be used for ANC synthesis and on-line identification of $C(z)$. The separation of $\tilde{p}_p$ and $z^{-N_1}\tilde{p}_s$ involves a notch filter $(1 - z^{-2N_1})/(1 - \gamma z^{-2N_1})$. Since the poles of the notch filter are damped zeros, its magnitude response is almost flat, implying a small dynamic range.

For short ducts with reflections from the duct outlet, (30) should be used. Substituting (10–12) respectively, (30) becomes

$$s_a \frac{-2z^{-N_1}}{C(z)} \left[\frac{1 - z^{-2N_1}}{1 - \gamma z^{-2N_1}} (w_p + w_r) - \frac{1 - z^{-2N_3}}{1 - \gamma z^{-2N_3}} w_r \right] \tag{34}$$

if $l_1 = l_2$. The above equation involves two notch filters $(1 - z^{-2N_1})/(1 - \gamma z^{-2N_1})$ and $(1 - z^{-2N_3})/(1 - \gamma z^{-2N_3})$. The numerators of the two notch filters are hidden in the operations $p_1 - p_2$ and $(p_2 z^{-N_3} - p_3)z^{-N_3}$ respectively. Choosing γ close to 1, one narrows the notches without increasing the dynamic range of the signal. The closer to 1 γ is, the closer to unity the transfer functions of the two notch filters become. As the result, the ANC signal can be approximated as

$$s_a \approx -[z^{-N_1}/C(z)]w_p,$$

which can be easily verified by a simple simulation program.

5.2. THE ERROR PATH

The focus of comparison is now directed to another common problem with feedforward ANC schemes—the unknown transfer characteristics of the sound-source effect. It must be measured via some experiments or identified by an adaptive algorithm as the performance of an ANC depends on accurate knowledge of such an effect [9, 11]. Elliot and Nelson modelled this transfer function by H_{sa} [6], while Munjal and Eriksson fit it with Z_{sa} [8]. It is included in the excitation path $C(z)$ in the present study. When an adaptive law is to be designed, the transfer function of the error path becomes a problem with the available feedforward ANC schemes. According to Munjal and Eriksson [8], the error path transfer function is given by

$$[Z_o \cos k_o l_d + \mathrm{j} Y_o \sin k_o l_d]/[Z_o \cos k_o(l_d + l_e) + \mathrm{j} Y_o \sin k_o(l_d + l_e)], \tag{35}$$

where Z_o is the radiation impedance of the duct outlet, l_e the distance from the antisound to the error sensor, and l_d the distance between the error sensor and the duct outlet.

Obviously, the transfer function of the error path (35) depends on Z_o which is not conveniently available. Although it is possible to apply the LMS and fit (35) with a linear difference equation, a pseudorandom signal has to be added to the antisound. As the result, the error sensor will pick up a signal mixture consisting of the cancellation error and the impulse response of the error path. There are difficulties separating the impulse response of the error path from the cancellation error, since both signals share the same frequency range. Besides, the pseudorandom signal is not cancelled, adding an annoying side effect to the ANC system.

The proposed system, however, does not have such a problem. With w_2^+ as the error signal, the transfer function of the error path is a simple delay factor and easy to identify. There is no need for the pseudorandom signal at all. The availability of w_s on the other hand, provides an output signal for a straightforward on-line identification of the excitation path $\hat{C}(z)$.

6. SIMULATION RESULTS

The proposed ANC is tested by simulating the acoustic field of a duct section of 10 m. A broadband noise signal enters the duct at $x = -5$ m while the antisound loudspeaker is placed at $x_s = 0{\cdot}0$ m. The ANC parameters are chosen to be $l_1 = l_2 = 1$ m and $l_3 = 0{\cdot}1$ m. The simulated outlet, at $x = 5$ m, radiates 10% of the sound energy out to the environment and reflects 90% back into the duct to form w_r.

In the simulation, the transfer function of the excitation path $C(z)$ is not available to the ANC system. Two separate LMS processes identify $\hat{C}(z)$ and $\hat{T}(z)$ respectively, using two FIR filters to model the estimated transfer functions. The adaptation processes minimize (25) and (26) by adjusting $\hat{C}(z)$ and $\hat{T}(z)$ respectively every 0·4 s.

Two types of incident noise signal are tested in the simulation, (1) a pseudorandom signal and (2) a periodic signal consisting of three frequency components. For the second case with a periodic incident noise, the simulation study also tested the ANC when the sensors are perfect, and when the sensors are contaminated by noise with a signal to noise ratio of 10:1.

For the first case, the system converges in 60 s of simulated time, which is equivalent to a propagation of 20 km at sound speed 340 m/s. It has been observed that the narrower the bandwidth of incident noise or smaller amount of reflection for the duct outlet, the faster the system converges. Figure 7 plots a snapshot of

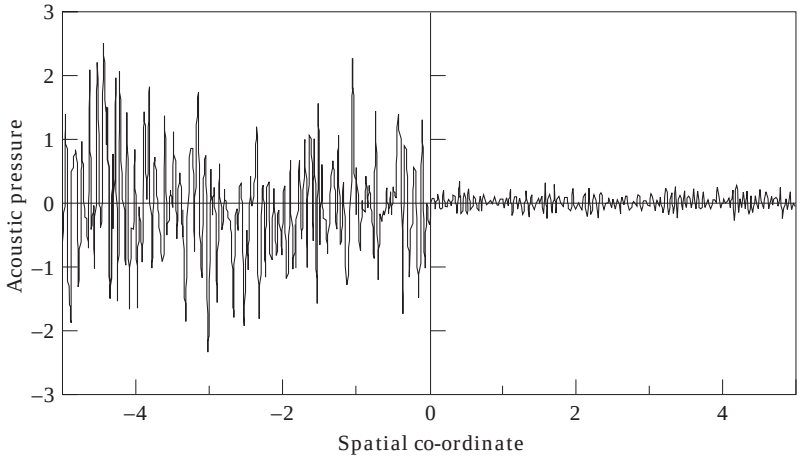

Figure 7. Simulated cancellation result of the ANC with pseudorandom incident noise.

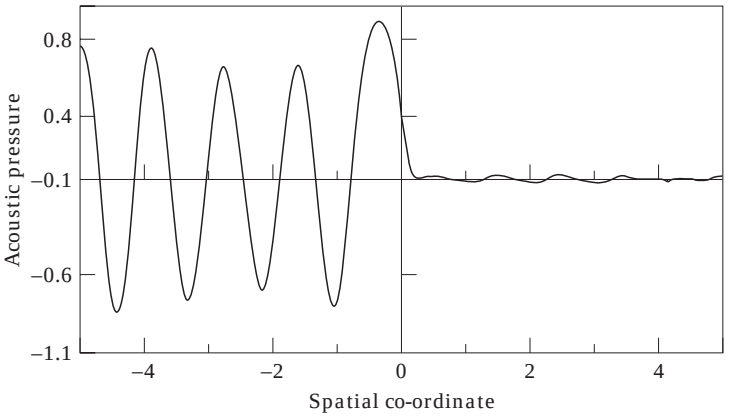

Figure 8. Numerically simulated cancellation result of the ANC using noise-free sensors.

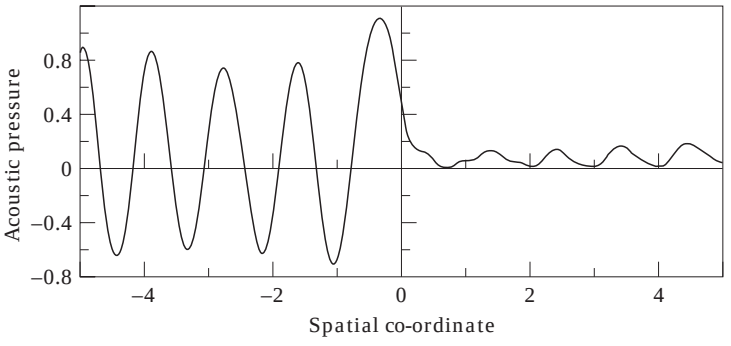

Figure 9. Numerically simulated cancellation result of the ANC using contaminated sensors.

the acoustic pressure signals (as a function of spatial co-ordinate x) in the duct after system convergence. For the second case, the convergence is much faster (in a couple of seconds). Figures 8 and 9 compared two snapshots of acoustic pressure in the duct taken at exactly the same instant from starting time. Figure 8 is the cancellation result by the ANC using noise-free sensors whereas Figure 9 shows the cancellation result by the ANC using contaminated sensors. The adaptation process seems robust with respect to the sensor noises. Yet the cancellation performances degrades significantly due to contamination.

The simulation results confirm the theory of the proposed ANC. A real implementation, however, depends on the quality and calibration of the hardware, such as the sensor, A/D and D/A converter, amplifier and loudspeaker. The linearity and frequency response of the hardware play important roles in the ANC, which were idealized in the simulation.

7. CONCLUSIONS

Feedforward cancellation is a popular approach for ANC in ducts. Its optimal performance depends on the knowledge of the excitation characteristics of the

antisound source. Such knowledge can be represented by a transfer function [6] or an acoustic impedance [8], which can be measured off-line or identified on-line. There remain some problems with on-line identification of the excitation path. These problems, in turn, depend on the transfer function of the error path, which is yet another unknown function to be identified.

The present approach simplifies transfer functions to time delay factors by separating pressure signals into the incident wave of noise, the reflected wave from the duct outlet, the cancellation error wave, and the antisound wave. An adaptive ANC scheme is proposed to avoid the pseudorandom signal while identifying the error path. Good performance of the proposed method is demonstrated by both analytical study and numerical simulations.

REFERENCES

1. M. R. Bai and C. Shieh 1995 *Journal of the Acoustical Society of America* **97**, 2664–2674. Active noise cancellation by using the linear quadratic Guassian independent model modal space control.
2. R. Clark 1995 *Journal of the Acoustical Society of America* **97**, 1710–1716. Active damping of enclosed sound fields through direct rate feedback control.
3. A. J. Hull, C. J. Radcliffe, M. Mikelavic and C. R. MacCluer 1991 *Journal of Vibrational Acoustics* **112**, 483–488. State space representation of the non-self-adjoint acoustic duct system.
4. A. J. Hull, C. J. Radcliffe and S. C. Southward 1991 *ASME Winter Annual Meeting* **91-WA-DSC-10**. Global active noise control of a one-dimensional acoust duct using a feed back controller.
5. Z. Wu, V. K. Varadan and V. V. Varadan 1995 *Journal of the Acoustical Society of America* **97**, 1078–1087. Active absorption of acoustic waves using state-space model and optimal control theory.
6. S. J. Elliott and P. A. Nelson 1984 *I.S.V.R. Technical Report* **127**, *Southampton*. Models for describing active noise control in ducts.
7. M. Bai and H. Chen 1996 *Journal of Sound and Vibration* **198**, 81–94. A modified H_2 feedforward active control system for suppressing broadband random and transient noise.
8. M. L. Munjal and L. J. Eriksson 1988 *Journal of the Acoustical Society of America* **84**, 1086–1093. An analytical, one-dimensional, standing-wave model of a linear active noise control system in a duct.
9. L. J. Eriksson and M. C. Allie 1988 *Journal of Sound and Vibration* **22**, 797–802. A practical system for active attenuation in ducts.
10. F. Orduuma-Bustamante and P. A. Nelson 1992 *Journal of the Acoustical Society of America* **91**, 2740–2747. An adaptive controller for active absorption of sound.
11. P. A. Nelson and S. J. Elliot 1992 *Active Control of Sound*. London: Academic Press.
12. J. Hu 1996 *ASME*, *Journal of Dynamic Systems*, *Measurement and Control* **118**, 372–378. Feedback and feedforward control strategy for active noise cancellation in ducts.
13. L. E. Kinsler, A. R. Frey, A. B. Coppens and J. V. Sanders 1992 *Fundamentals of Acoustics*. New York: Wiley.